AGU PUBLICATIONS

JGR

Journal of Geophysical Research: Solid Earth

RESEARCH ARTICLE
10.1002/2016JB013150

Key Points:
- A gas composition precursor to eruptions is identified
- Changes in gas compositions are associated with transitions in eruptive processes
- Magma depth and volume are constrained

Supporting Information:
- Supporting Information S1
- Table S2
- Data Set S1
- Data Set S2

Correspondence to:
J. M. de Moor,
maartenjdemoor@gmail.com

Citation:
de Moor, J. M., et al. (2016), Turmoil at Turrialba Volcano (Costa Rica): Degassing and eruptive processes inferred from high-frequency gas monitoring, *J. Geophys. Res. Solid Earth*, *121*, 5761–5775, doi:10.1002/2016JB013150.

Received 5 MAY 2016
Accepted 1 JUL 2016
Accepted article online 5 JUL 2016
Published online 28 AUG 2016

Turmoil at Turrialba Volcano (Costa Rica): Degassing and eruptive processes inferred from high-frequency gas monitoring

J. Maarten de Moor[1,2,3], A. Aiuppa[3,4], G. Avard[1], H. Wehrmann[5], N. Dunbar[6], C. Muller[1,7], G. Tamburello[3], G. Giudice[4], M. Liuzzo[4], R. Moretti[8], V. Conde[9], and B. Galle[9]

[1]Observatorio Vulcanológico y Sismológico de Costa Rica, Universidad Nacional, Heredia, Costa Rica, [2]Department of Earth and Planetary Sciences, University of New Mexico, Albuquerque, New Mexico, USA, [3]Dipartimento DiSTeM, Università di Palermo, Palermo, Italy, [4]Istituto Nazionale di Geofisica e Vulcanologia, Sezione di Palermo, Palermo, Italy, [5]GEOMAR Helmholtz Centre for Ocean Research Kiel, Kiel, Germany, [6]New Mexico Bureau of Geology & Mineral Resources, Earth and Environmental Science Department, Socorro, New Mexico, USA, [7]School of Earth Sciences, University of Bristol, Bristol, UK, [8]Dipartimento di Ingegneria Civile Design, Edilizia e Ambiente Seconda Università degli Studi di Napoli, Naples, Italy, [9]Department of Earth and Space Sciences, Chalmers University of Technology, Göteborg, Sweden

Abstract Eruptive activity at Turrialba Volcano (Costa Rica) has escalated significantly since 2014, causing airport and school closures in the capital city of San José. Whether or not new magma is involved in the current unrest seems probable but remains a matter of debate as ash deposits are dominated by hydrothermal material. Here we use high-frequency gas monitoring to track the behavior of the volcano between 2014 and 2015 and to decipher magmatic versus hydrothermal contributions to the eruptions. Pulses of deeply derived CO_2-rich gas ($CO_2/S_{total} > 4.5$) precede explosive activity, providing a clear precursor to eruptive periods that occurs up to 2 weeks before eruptions, which are accompanied by shallowly derived sulfur-rich magmatic gas emissions. Degassing modeling suggests that the deep magmatic reservoir is ~8–10 km deep, whereas the shallow magmatic gas source is at ~3–5 km. Two cycles of degassing and eruption are observed, each attributed to pulses of magma ascending through the deep reservoir to shallow crustal levels. The magmatic degassing signals were overprinted by a fluid contribution from the shallow hydrothermal system, modifying the gas compositions, contributing volatiles to the emissions, and reflecting complex processes of scrubbing, displacement, and volatilization. H_2S/SO_2 varies over 2 orders of magnitude through the monitoring period and demonstrates that the first eruptive episode involved hydrothermal gases, whereas the second did not. Massive degassing (>3000 T/d SO_2 and $H_2S/SO_2 > 1$) followed, suggesting boiling off of the hydrothermal system. The gas emissions show a remarkable shift to purely magmatic composition ($H_2S/SO_2 < 0.05$) during the second eruptive period, reflecting the depletion of the hydrothermal system or the establishment of high-temperature conduits bypassing remnant hydrothermal reservoirs, and the transition from phreatic to phreatomagmatic eruptive activity.

1. Introduction

Magmatic eruptions at previously dormant volcanoes are often preceded by phreatic eruptions [e.g., *Barberi et al.,* 1992]. Identifying the transition from phreatic to phreatomagmatic behavior is of paramount importance in hazard assessment during an evolving volcanic crisis as this change reflects the establishment of conduits directly connecting rising magma with the surface [e.g., *Nakada et al.,* 1995; *Suzuki et al.,* 2013]. The traditional method of defining this transition involves recognition of juvenile material in ash products. This approach involves detailed and time-consuming compositional and textural analysis of complex mixed ash samples that is difficult to accomplish fast enough for monitoring purposes during rapidly evolving volcanic crises [e.g., *Cashman and Hoblitt*, 2004; *Suzuki et al.,* 2013]. Moreover, distal ashes from phreatic and phreatomagmatic eruptions tend to be very fine grained; thus, samples collected at safe distances are also challenging to work with for component analysis. Ultimately, it is exceedingly difficult to ascertain whether glassy clasts in multicomponent ash represent fresh magma arriving at the surface or are derived from previously erupted (or shallowly intruded) material remobilized by explosive blasts, especially if the fresh material has similar composition to previous eruptive products [e.g., *Pardo et al.,* 2014].

Given the remarkable compositional dissimilarity between magma-derived gas and hydrothermal gases, gas monitoring can potentially provide invaluable insights into the processes causing unrest [e.g., *Chiodini et al.,* 2015;

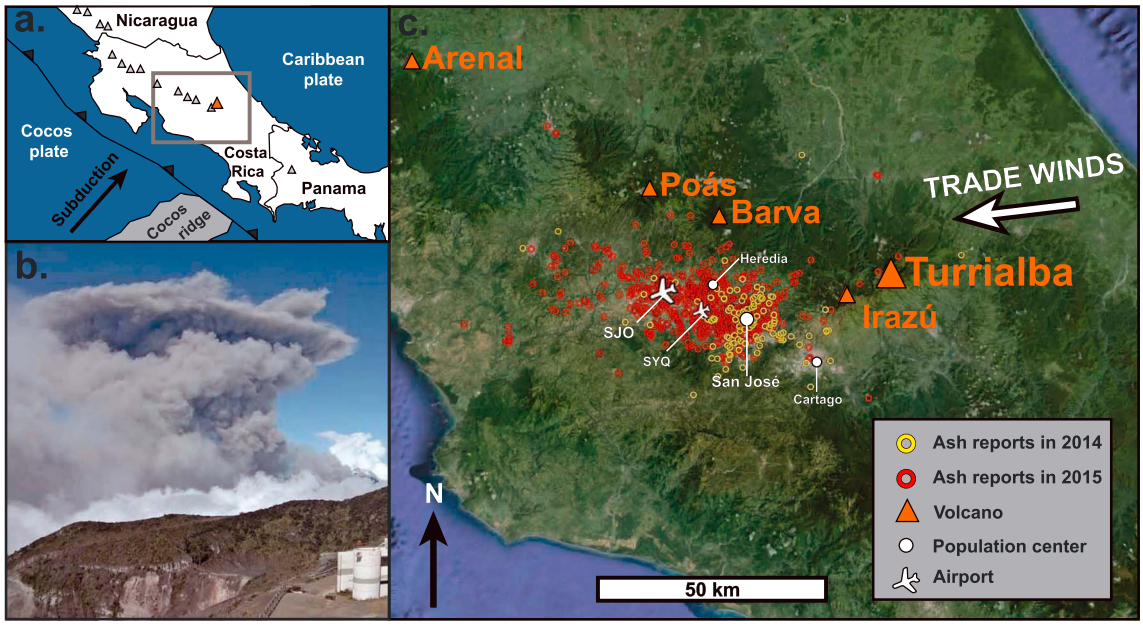

Figure 1. (a) Tectonic setting of Turrialba Volcano (orange triangle). Grey triangles indicate other volcanoes of the Central American Arc, and the grey box indicates the area shown in Figure 1c. (b) Explosive eruption at Turrialba on 12 March 2015, as captured by an OVSICORI webcam located on the summit of Irazú Volcano. (c) Location map of Turrialba Volcano in Costa Rica relative to the cities and airports (SJO: San José International Airport and SYQ: Tobias Bolaños International Airport) of the densely populated Central Valley, as well as volcanoes of the Cordillera Central. Hollow circles indicate reports received at OVSICORI of ash fall in 2014 (yellow) and in 2015 (red).

de Moor et al., 2016; *Giggenbach et al.,* 1990; *Vaselli et al.,* 2010]. However, continuous long-term instrumental records of gas compositional variations at the quiescence-to phreatic- to magmatic transition are essentially absent in the geological literature.

Here we report on variations in gas ratios measured in situ using a fixed multi-component gas analyzer (multi-GAS) and gas fluxes measured by scanning differential optical absorption spectrometer (DOAS) at Turrialba Volcano (Costa Rica; 10.0183°N, 83.7646°W; 3340 m elevation) during an ongoing reawakening process and volcanic crisis. Recent activity has involved frequent ash emission events that have opened new vents and represent the latest and most advanced manifestation of the transition from hydrothermal to magmatic activity. Turrialba Volcano is located ~30 km upwind of San José (Figure 1; the capital of Costa Rica) and ~50 km upwind of San José International Airport (SJO). Thus, even small eruptions from this volcano threaten the quality of life for approximately three million people (~60% of the Costa Rican population lives in the central valley) and the economic heart of the country.

2. Background and Geologic Setting

The name "Turrialba" may be derived from the Latin for "white tower," probably referring to the condensed gas plume visible from ships bearing European settlers to the Caribbean coast [*Alvarado*, 2009]. Turrialba and Irazú (Figure 1) Volcanoes share a common base covering an area of roughly 60 km by 45 km, with their summit craters just 10 km apart. Together they form the largest and southernmost active volcanic edifice on the Central American Arc [*Carr and Stoiber*, 1990]. The subduction of the Cocos plate beneath the Caribbean plate is low angle (~40°) and high temperature in this region, due to the subduction of the buoyant and hot Cocos ridge [e.g., *Peacock et al.,* 2005, Figure 1]. In southern Costa Rica and Panama, flat slab subduction (<30°) causes uplift of the Talamanca Mountains (3800 m) without recent active volcanism. The magma source region feeding Turrialba and Irazú Volcanoes is similar, in that the two show evidence of both arc-like and oceanic island basalt-like signatures in terms of trace elements and radiogenic isotopes [*Benjamin et al.,* 2007; *Di Piazza et al.,* 2015]. The enriched character of magmas in southern Costa Rica most likely originates from the subduction of seamounts formed by the Galapagos hot spot [*Gazel et al.,* 2009].

Variations in volatile chemistry along the Central American Arc reflect along-arc changes in the influence of mantle versus slab-derived fluids. In general, the volcanoes of Costa Rica show more mantle source and less sedimentary signature than the rest of the arc. Turrialba has the highest $^3He/^4He$ value (Rc/Ra = 8.1) in the region [*Di Piazza et al.,* 2015], consistent with its slightly "back-of-the-arc" location and strong mantle signature. The chemical and isotopic compositions of C and He in fumarolic gas emissions from Turrialba and Irazú suggest that these volatiles have a greater mantle signature at these volcanoes in comparison with the rest of the arc [*Shaw et al.,* 2003]. Along-arc trends in CO_2 content of melt inclusions [*Wehrmann et al.,* 2011] and CO_2/SO_2 in plume gas emissions [*Aiuppa et al.,* 2014] both show that the southernmost volcanoes in Central America are also relatively carbon poor. Interestingly, though Turrialba-Irazú volatile systematics are consistent with strong mantle and weak slab fluid signatures, water contents in basaltic Irazú melt inclusions show typical arc contents of ~3 wt % [*Benjamin et al.,* 2007]. Similarly, new S isotope data for Turrialbas gas plume (samples collected and analyzed using the methods of *de Moor et al.* [2013b]; see supporting information) show a range of values between +0.2‰ and +7.3‰ with an average of +3.4 ± 0.5‰ [*de Moor et al.,* 2013a], which falls closer to typical values measured in high-temperature arc gases (~ + 5‰) than to values observed in purely mantle-derived gases (~ + 0‰) [*de Moor et al.,* 2013b; *Oppenheimer et al.,* 2012].

3. Current Eruptive Activity

The reactivation of Turrialba has been a decades-long process. The last magmatic eruption occurred in 1864–1866, which was preceded by fumarolic degassing and phreatic activity [*Di Piazza et al.,* 2015; *González et al.,* 2015; *Reagan et al.,* 2006]. Seismic swarms, increasing degassing intensity, and changes in fumarolic gas chemistry were the first indications of unrest in the late twentieth century [*Martini et al.,* 2010; *Vaselli et al.,* 2010], heralding the end of ~120 years of repose. Seismicity peaked in 2009 and 2010 [*Martini et al.,* 2010], and SO_2 flux reached a maximum of ~3500 T/d in mid-2009 [*Conde et al.,* 2013]. The first phreatic eruption at Turrialba occurred on 5 January 2010, which formed a moderate- to high-temperature fumarolic vent (300°C to 600°C) on the inner west crater rim that allowed open system degassing immediately after the vent-opening eruption [*Campion et al.,* 2012]. Further phreatic eruptions in January 2012 opened a new high-temperature vent (500°C to 800°C) on the southeast rim of the west crater. On 21 May 2013, both vents (located about 300 m apart) emitted ash simultaneously.

A new and more vigorous phase of eruptive activity began on 29 October 2014 with the most energetic blast to date and collapse of the eastern wall of the west crater. Ash emissions continued for 2 weeks, and another more energetic explosion occurred on 9 December. This eruptive period was followed by 3 months of strong quiescent degassing and seismicity. Eruptive activity resumed on 8 March 2015 with at least 20 days of intermittent ash emissions (>32 events) until 18 May. The most energetic explosions during this period occurred on 12 March 2015 (Figures 1 and 2) and 7 April 2015. Isolated ash emission events took place in June and August 2015.

A new period of frequent low-energy ash emissions took place in October 2015, with further passive ash emissions in early 2016. Frequent small explosive eruptions and persistent ash emissions resumed again on 30 April 2016 and are ongoing at the time of writing. Small intracaldera pyroclastic flows have occurred since 2015, and the first pyroclastic flow to leave the crater occurred in May 2016. The ash emissions periods pertinent to this work (2014–2015) represent two distinct episodes of eruptive activity (Figure 2; degassing phases 3 and 6).

The 2014 to present eruptions have blanketed the central valley in fine ash on at least 30 days since 29 October 2014, caused air traffic closures in five instances, closures of schools, and resulted in evacuations of the local farming communities. The ashes from the second eruptive episode (March–May 2015) had greater societal impact (Figure 1c), with reports of ash fall as far as 100 km from the volcano, and five episodes resulting in flight cancelations. The 12 March 2015 eruption, in particular, (Figure 1b) had significant impact, causing the closure of 12 schools, the evacuation of farms within 2 km of the crater, and causing 111 flights to be canceled at SJO International Airport, affecting ~7000 passengers.

4. Methods

We installed a fixed multi-GAS station with data telemetry on the outer southwest rim of the active west crater of Turrialba in February 2014, capturing a significant change in activity from passive degassing with very sparse isolated ash emissions (~1 event per year) pre-2014 to much more frequent eruptive activity

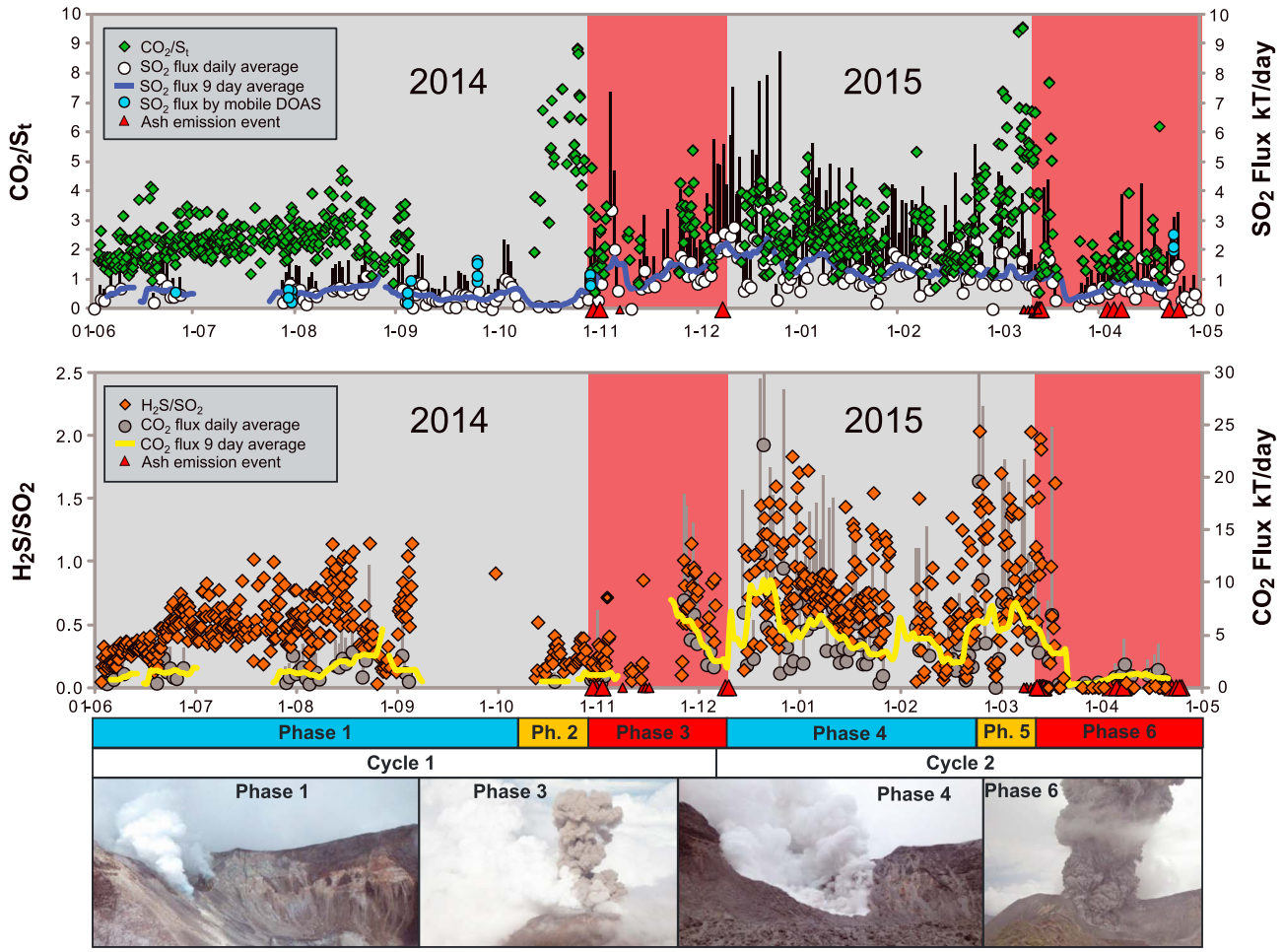

Figure 2. Time series of gas fluxes and gas compositions at Turrialba Volcano from June 2014 to May 2015. Daily mean flux values are indicated by circles and associated bars indicate the 75th percentile of individual days. Blue and yellow lines indicate 9 day moving average of the gas flux. Diamonds show gas ratios as measured by permanent multi-GAS station, and red triangles show the occurrence of explosions (larger triangles) or ash emissions (small triangles). Upper time series plot shows SO_2 flux measured by scanning DOAS and CO_2/S_{total} where S_{total} represents $SO_2 + H_2S$. Importantly, clear peaks occur in CO_2/S_{total} weeks prior to both eruptive periods. The highest SO_2 fluxes occurred after the vent-opening eruptions in 2014 followed by a relatively steady decrease. Lower time series plot shows CO_2 flux (calculated based on SO_2 flux and CO_2/SO_2) and H_2S/SO_2 as measured by multi-GAS. Importantly, H_2S/SO_2 drops to purely magmatic values after the first series of eruption in 2015. H_2S tracks the influence of hydrothermal fluids at Turrialba, and the time series shows that the peak in CO_2/S_t prior to the late 2014 eruptions has weak hydrothermal character. Six degassing phases are recognized based on variations in the gas fluxes and compositions (bottom axis). Phases 1 and 4 show stronger hydrothermal influence with relatively high H_2S/SO_2. Phases 2 and 5 precede the eruptive phases and display high CO_2/S_t with variable hydrothermal influence. Phases 3 and 6 are defined by eruptive activity and show low CO_2/S and low H_2S/SO_2 immediately after eruptions. Note that each individual phase shows unique combinations of gas flux and compositional characteristics. Photos from left to right displaying typical activity for the indicated phases: Quiescent degassing during phase 1 prior to the explosive eruption at 11:35 pm on 29 October 2014. Ash emission event on 30 October 2014 (photo by Federico Chavarria). Intense degassing occurred in the months after the 29 October eruption during phase 4. Ash eruption during phase 6 on 4 May 2015 as captured by the OVSICORI webcam.

following the 29 October 2014 eruption. The multi-GAS instrument measures gas concentrations of SO_2, H_2S, CO_2, and H_2O at a rate of 0.1 Hz for 30 min 4 times a day with data telemetered to Observatorio Vulcanológico y Sismológico de Costa Rica (OVSICORI) in near real time. Gas ratios (molar H_2S/SO_2, CO_2/SO_2, and H_2O/SO_2) are derived from linear regression through the concentration data and are independent of mixing with air [*Aiuppa et al.,* 2007, 2009, 2014; *de Moor et al.,* 2016], allowing us to derive a time series of gas compositions (Figure 2). Errors in gas ratios as measured by multi-GAS are $<20\%$ [*de Moor et al.,* 2016] and are far less than the large (order of magnitude scale) variations observed in the data. The multi-GAS instrument was calibrated in the lab periodically (on 30 May 2014, 14 September 2014, and 27 January 2015) and the slope and intercept of the calibration curves varied by less than 10% during the course of the study.

The emission rate of SO_2 from Turrialba is monitored by scanning UV spectrometer systems installed through the Network for the Observation of Volcanic and Atmospheric Change project [*Conde et al.,* 2013; *Galle et al.,* 2010]. These instruments are located about 2 km from the summit downwind of the volcano and scan the sky continuously during daylight hours to measure the integrated absorption of UV light by SO_2 in the plume. Flux is estimated based on the integrated SO_2 column amounts from 50 measurements taken at 3.6° steps to cover 180° scans of the sky. Plume height is obtained from triangulation by the two stations or webcam images when triangulation cannot be made, and the wind speed and direction is measured by a weather station located at the summit of the volcano [*Conde et al.,* 2013]. Multiplication of the SO_2 emission rates with gas ratios (converted from molar ratios to mass based concentration ratios) expressed with SO_2 as the denominator result in estimations of the fluxes of CO_2, H_2S, and H_2O.

We also conducted electron microprobe analyses of magmatic clasts erupted during the 1864–1866 eruption to compare their composition to fresh glassy clasts erupted in the recent eruptions. Melt inclusions and matrix glass from these deposits were analyzed. Our ash sample collected from the 29 October 2014 eruption contains fine hydrothermally altered material, lithics, and ~10% fresh glassy and vesicular material that is suspected to be juvenile. The latter component was analyzed via microprobe for major elements, S, Cl, and F. Full methods and sample details are reported in the supporting information.

5. Results and Discussion

5.1. Changes in Degassing During Volcano Reactivation

Our high-frequency time series of gas compositions and fluxes (Figure 2) allows us to observe in unprecedented detail the degassing processes involved during reactivation of a previously dormant volcanic system. In this section, we highlight the most important observations of the changes in degassing during the reactivation of Turrialba. We recognize six phases (Figure 2) within two cycles of degassing and eruption during the period between June 2014 to May 2015, which we group as such based on distinguishing features in the gas compositions.

During quiescent degassing phase 1 the system was relatively stable, with low gas fluxes and hydrothermally influenced gas composition, as demonstrated by the presence of H_2S (Figure 3) (we here assume $H_2S/SO_2 > 0.3$ to be a relatively unambiguous indicator of hydrothermal interaction; Figure 3). Daily mean SO_2 flux values were typically less than 1000 T/d with CO_2/S_t of 1 to 4 (S_t refers to total sulfur, i.e., $SO_2 + H_2S$), moderate H_2S/SO_2 of 0.2 to 0.7, and H_2O/SO_2 of 10 to 40. In the weeks prior to the 29 October eruption (phase 2), CO_2/S_t increased dramatically, up to values of 7–9. Importantly, this precursory gas signal occurred in parallel with a decrease of H_2S/SO_2 down to 0.05–0.3, excluding a hydrothermal origin. Interestingly, both SO_2 and CO_2 fluxes are low during this period, suggesting that the conduits connecting the shallower magmatic system to the surface were less permeable to gas.

The CO_2/S_t values dropped in the hours prior to the 29 October eruption and remained low through the first eruptive period (phase 3). The hydrothermal component (H_2S) increased through phase 3, from $H_2S/SO_2 \sim 0.2$ to ~0.7. Significantly, the gas fluxes increase dramatically only after the 9 December eruption (phase 4), coupled with further increase in H_2S/SO_2 to values > 1.5.

A second peak in CO_2/S_t (~5 to 9.5) occurred in the first 2 weeks of March 2015 (phase 5), which heralded the onset of eruptive activity starting on 8 March. In comparison to phase 2, phase 5 displays much higher H_2S/SO_2 (0.8–2) and higher SO_2 and CO_2 fluxes. A series of low-energy ash emissions on 8–11 March occurred prior to more energetic blasts starting on 12 March. The gas composition changed dramatically to low CO_2/SO_2 (1–2) and very low H_2S/SO_2 (<0.1) with the transition to more energetic eruptions (phase 6).

5.2. Glass Compositions: The Debate of New Versus Old Magma

Table 1 and Figure 4a compare the composition of most pristine matrix glasses from the 29 October 2014 eruption with the 1864–1866 eruption, showing that the major element compositions are indistinguishable within the variability observed in the samples. Both the 1864–1866 glasses and the allegedly juvenile clasts have compositions falling between basaltic andesite and trachyandesite (Figure 4a and Table S2 and Figures S1 in the supporting information for petrologic results and discussion). We believe that at least some of these fresh-looking glassy and vesicular clasts represent true juvenile material; however, it is difficult to

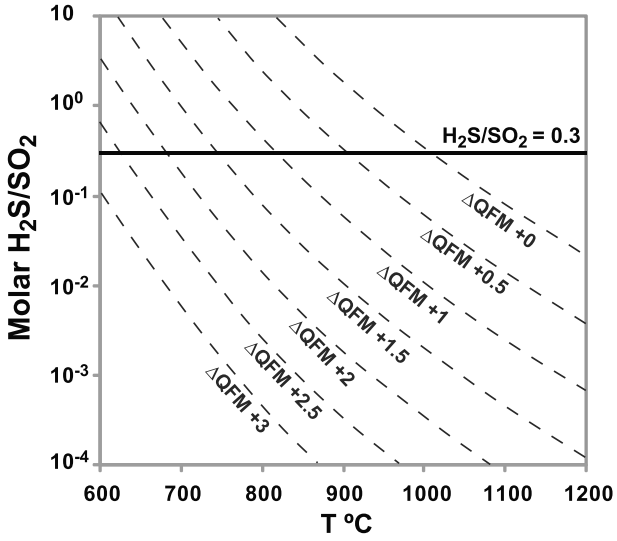

Figure 3. Plot of modeled H_2S/SO_2 as a function of temperature and oxygen fugacity (fO_2), at 1 bar pressure for a volcanic gas composition containing 95% H_2O. The equilibration fO_2 of the Turrialba gas emissions was estimated by *Moussallam et al.* [2014] to be between ΔQFM +1.5 and +3, and the temperature of Turrialba gas vents has been between 600°C and 800°C prior to the October 2014 eruption (robust T measurements have not been possible thereafter). Thus, at reasonable fO_2 and temperature conditions for the period of multi-GAS measurements (ΔQFM > +1.5 and T > 600°C) magmatic gas emissions are strongly dominated by SO_2. For the purposes of discussion, we assume that $H_2S/SO_2 > 0.3$ reflects relatively unambiguous contribution of hydrothermal H_2S to gas emissions, acknowledging that this value is rather arbitrary. See *de Moor et al.* [2013a, 2013b] for full modeling methods and relevant references.

ascertain with certainty whether these clasts were molten at the time of eruption and represent the composition of the magma driving the current unrest.

Some of the fresh-looking glassy clasts in our ash sample from the 29 October 2014 eruption show anomalously high F contents (Figure 4b; 2 wt% to 5.5 wt%), which cannot be a primary magmatic signature. Rather, the clasts with very high F content are interpreted to reflect "cryptic" alteration. This process probably occurs below the glass transition temperature, whereby HF-rich gas exsolved at shallow levels in the magmatic plumbing system interact with recently emplaced (though difficult to quantify when) quenched and degassed magma [*Reagan et al.,* 2011]. However, another possibility is that the alteration occurs very rapidly during the eruption itself due to interaction with HF-rich gas in the subaerial environment [*Spadaro et al.,* 2002].

The crux of the argument as to whether the fresh-looking clasts are "juvenile" or not lies in quantifying when liquid melt quenched to glass and how fast alteration (cryptic or obvious) processes occur. Presently, not enough constraints on this timing are available to determine with confidence whether the fresh-looking clasts represent the eruption of new magma after rising rapidly from the mantle through the crust [e.g., *Ruprecht and Plank*, 2013] or remobilization of old (or even recently emplaced but not erupted) magmatic material entrained during hydrothermally driven eruptions [*Cashman and Hoblitt*, 2004; *Giggenbach et al.,* 1990; *Pardo et al.,* 2014; *Suzuki et al.,* 2013; *Williams et al.,* 1986]. Furthermore, newly intruded but unerupted magma can reactive overlying magma through the introduction of volatiles and heat, causing eruption of magma that may not be the direct parent of the associated emitted volatiles [e.g., *Claiborne et al.,* 2010; *Larsen et al.,* 2010].

Table 1. Comparison Between Compositions of Matrix Glass Erupted in 1864–1866 and That From the 29 October 2014 Eruption[a]

	1864–1866 Matrix Glass ($n = 15$)		2014 Matrix Glass ($n = 11$)	
	Average	SD	Average	SD
SiO_2	56.02	0.56	56.98	1.27
TiO_2	1.51	0.20	1.80	0.17
Al_2O_3	16.44	1.01	15.36	0.84
FeO	8.59	0.85	9.21	0.52
MnO	0.18	0.05	0.18	0.03
MgO	3.45	0.31	3.45	0.51
CaO	7.39	0.82	6.31	0.57
Na_2O	3.52	0.65	3.12	1.16
K_2O	2.31	0.41	2.55	0.48
P_2O_5	0.61	0.10	0.71	0.14
S ppm	93	104	175	98
Cl ppm	1108	208	1255	679
F ppm	887	421	1550	748
Total	100.2		100.0	

[a]The compositions are essentially indistinguishable within the observed variability. SD refers to the standard deviation observed in the data.

Figure 5 compares magma chemistry from Turrialba (1864–1866 eruption) and Irazú (1963–1965 eruption). The two volcanoes show parallel degassing-crystallization trends, with Irazú falling at slightly

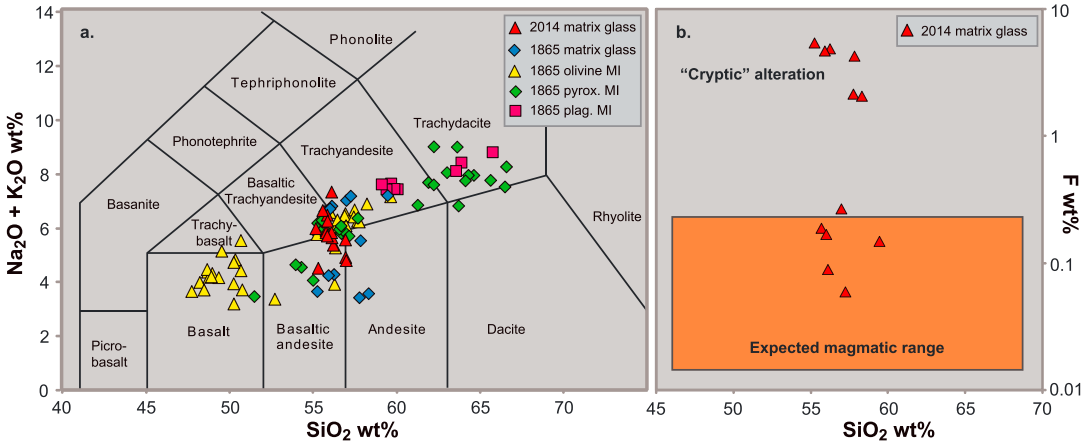

Figure 4. (a) Total alkalis versus silica classification diagram comparing the composition of fresh-looking clasts in the 29 October 2014 ash (2014 matrix glass) with 1864–1866 magma compositions (1865 matrix glass, olivine melt inclusions, pyroxene melt inclusions, and plagioclase melt inclusions). (b) Fluorine concentration in wt % versus silica. Some of fresh-looking clasts in the 29 October 2014 ash show anomalously high F contents, interpreted to reflect cryptic alteration due to preeruptive (but post cooling below glass transition temperature) interaction with F-rich gas/liquid.

more K-rich compositions. Interestingly, plagioclase- and pyroxene-hosted melt inclusions in both systems show a large number of inclusions with higher K_2O than their respective matrix glasses, suggesting entrainment of a significant portion of old, previously degassed magma in past eruptive products.

The composition and morphology of the fresh-looking clasts from one ash sample (29 October 2014 eruption) alone cannot fully or adequately resolve the key question for monitoring of whether "new" magma is involved in the present eruptions or not. While magma petrology/geochemistry/texture all provide rather equivocal results, with terminology becoming problematic as the discussion evolves, the short-term variations in gas compositions we observed at Turrialba (Figure 2) require rapidly changing volatile sources and conditions of degassing (i.e., pressure of gas exsolution from melt) over monitoring time scales and therefore shed light into the processes driving the volcano's current and evolving eruptive activity.

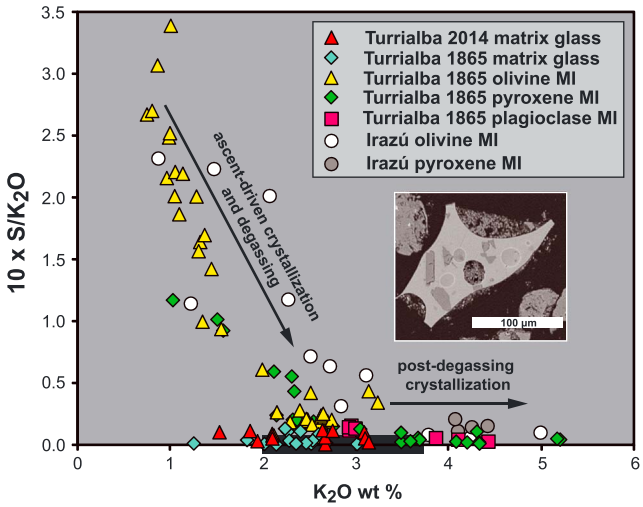

Figure 5. Plot of $10 \times S/K_2O$ versus K_2O with 2014 matrix glasses, 1865 melt inclusions and melt glasses, and melt inclusions from nearby Irazú Volcano. Olivine-hosted melt inclusions (yellow triangles) from the 1865 eruption are sulfur rich and K_2O poor, representing primitive undegassed melt. Matrix glasses from both 1865 and 2014 eruptions have essentially the same composition and have degassed almost all of their sulfur. The inset backscattered electron image shows a fresh-looking glassy shard (with adhered fine ash) erupted in October 2014 that is suspected to be juvenile. Interestingly, a significant group of pyroxene- and plagioclase-hosted melt inclusions from the 1865 eruption have higher K_2O than the Turrialba matrix glasses and are degassed. Irazú melt inclusions (data from *Benjamin et al.* [2007] and *Wehrmann et al.* [2011]) form a parallel trend to the Turrialba glasses. The black bar along the *X* axis shows the K_2O content of Irazú matrix glasses [*Alvarado*, 1993], again overlapping with Turrialba compositions but extending to higher K.

5.3. Degassing Sources and Processes

Each of the six phases of degassing (Figure 2) has unique characteristics in terms of gas composition and emission rate. Perhaps most importantly, high CO_2/S_{total} precedes both eruptive episodes, showing promise of a precursory signal useful in eruption forecasting. High CO_2/S_{total} (5–9) persisted for 2 weeks prior to the energetic eruption of 29 October 2014 and increased again 5 days prior to resumed onset of ash

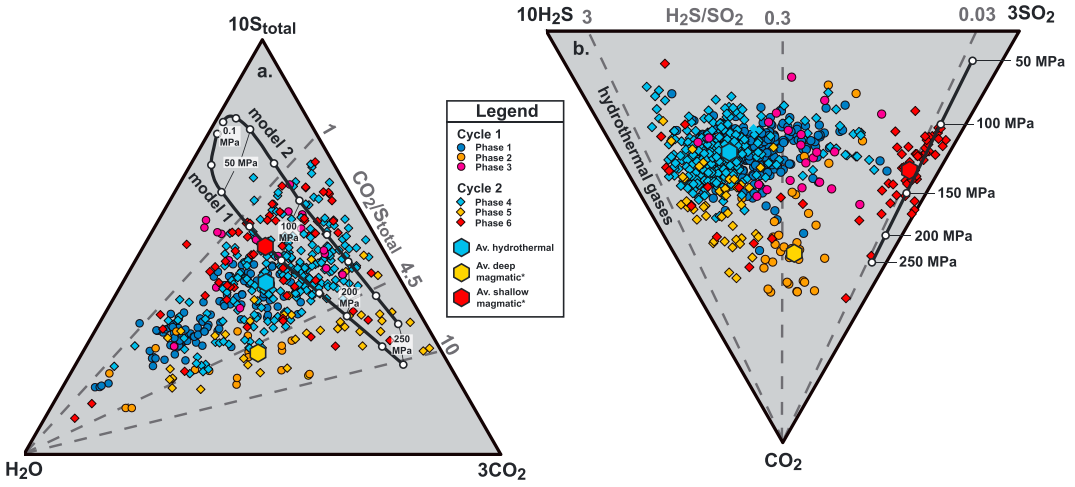

Figure 6. Triangular plots distinguishing gas sources and degassing trends. (a) S_{total}-H_2O-CO_2 and (b) H_2S-SO_2-CO_2. (c) A conceptual model for the Turrialba plumbing system based on the gas compositions. In Figure 6a, the only periods that show CO_2/S_{total} compositions greater than 4.5 are the precursory periods (yellow orange symbols; phases 2 and 5) to eruptive periods (phases 3 and 6), and emissions during the initial part of the phase 6 eruptive period (Figure 2). Decompression degassing models [*Moretti et al.,* 2003] are shown as solid black lines with pressure varied from 250 MPa to 0.1 MPa. Initial undegassed melt composition is based on melt inclusion data (see supporting information Tables S2 and S3 for details) from the 1864–1866 eruption at Turrialba (for major elements and S; supporting information Table S2), as well as the available data for CO_2 and H_2O contents from nearby Irazú Volcano [*Benjamin et al.,* 2007; *Wehrmann et al.,* 2011]. The starting composition for Model 1 has 3 wt % H_2O, 200 ppm CO_2, 2000 ppm S, whereas model 2 starting composition has 2.5 wt % H_2O, 200 ppm CO_2, 2000 ppm S. In Figure 6a, high H_2O compositions are mostly associated with gases from hydrothermal and precursory phases indicating meteoric (hydrothermal) water input. Apart from the high H_2O compositions, the gases are consistent with magmatic degassing between >250 MPa and ~100 MPa. In Figure 6b, only model 1 is shown as exsolved gas compositions are recalculated to surface conditions (QFM +3, 0.1 MPa, 650°C) [*Moussallam et al.,* 2014]. At these conditions the H_2S/SO_2 ratio is fixed at ~0.02 independent of original H_2S/SO_2 composition, which is a function of T, P, H_2O, and fO_2. High H_2S/SO_2 ratios are indicative of hydrothermal fluid input or reactions converting SO_2 to H_2S in the reducing hydrothermal environment. Thus, in both plots deviations from the modeled gas compositions can adequately be explained by hydrothermal input of H_2O and H_2S. Importantly, the H_2S/SO_2 clearly distinguishes hydrothermal phases 1 and 4 and magmatic degassing, which is characterized by $H_2S/SO_2 < 0.3$. Average hydrothermal, deep magmatic, and shallow gas compositions are shown as hexagons. The deep magmatic and shallow magmatic averages are calculated using phase 2 and phase 6 gas compositions only, because phases 3 and 5 show significant hydrothermal overprint.

emissions in March 2015. *Aiuppa et al.* [2007] similarly observed high CO_2/SO_2 prior to eruptions at Etna, suggesting that precursory short-term pulses in CO_2 may be a common occurrence at many volcanoes. Another striking feature of our gas composition time series is the abrupt order of magnitude scale change in H_2S/SO_2 that coincided with the 12 March 2015 eruptions. To our knowledge, this is the first report of dramatic short term changes in H_2S/SO_2 correlated with eruptive activity.

In order to explain the sources and processes responsible for the tumultuous variations in composition, we have conducted analysis of the CO_2-SO_2-H_2S-H_2O system (Figure 6), from which we propose three dominant sources or types of gas emissions: (1) deep CO_2-rich magmatic gas,(2) SO_2-rich gas from shallow magmatic degassing, and (3) H_2S-rich hydrothermal gas. We argue that the changes in gas compositions are driven by pulses of magma rising through the crust, and in this section we track the degassing pathways from deep to shallow levels (Figure 4).

5.3.1. Deep Magmatic Gas

Pulses of CO_2-rich gas are observed before both the October–December 2014 and the March–May 2015 eruptive episodes (Figures 2 and 6a). The high CO_2/S_t ratio signature of this gas precursor only occurs in the weeks to days prior to energetic explosive eruptions and is not associated with other periods (Figure 6), implying a distinct gas source. Based on results of decompression degassing models (Figure 6), we interpret the pulses of CO_2-rich gas as due to degassing of intruding magma batches arriving at deep to midcrustal levels (Figure 7), where CO_2 is preferentially exsolved from the melt over higher solubility S [e.g., *Aiuppa et al.,* 2007; *Baker and Moretti*, 2011; *Giggenbach*, 1996; *Holloway and Blank*, 1994; *Lesne et al.,* 2011]. Results of decompression degassing modeling, in particular, suggest that CO_2-rich gases correspond to the magmatic gas exsolved at

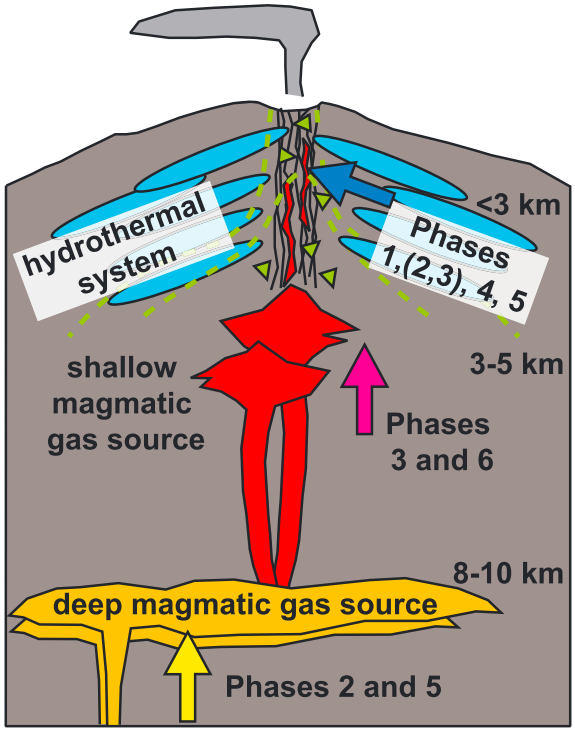

Figure 7. Conceptual model of Turrialba Volcano showing the plumbing system as envisioned from gas compositions and modeling. Pulses of new magma arrive at midcrustal depths (8–10 km) during phases 2 and 5, producing CO_2-rich gas pulses and destabilizing a lower magma reservoir. Shortly thereafter, magma, volatiles, and heat are injected to the shallow magmatic system, triggering phreatic and phreatomagmatic eruptions. An extensive hydrothermal system contributes volatiles and modifies magmatic gas compositions mostly during phases 1, 4, and 5 and to lesser extent during phases 2 and 3. Phase 3 eruptions (particularly the 29 October 2014 event) ruptured hydrothermally sealed breccia (green triangles) previously sealed at chemical and thermal interfaces between magmatic vapor and hydrothermal liquid zones, allowing massive degassing of hydrothermally stored volatiles during stage 4.

equilibrium conditions from melt at 200–250 MPa or depths of 8–10 km (Figure 6) [*Moretti et al.,* 2003]. An additional key piece of evidence leading to this interpretation is the fact that edifice inflation is an ongoing process at Turrialba (Figure S2), supporting the scenario of magma intrusion.

5.3.2. Shallow Magmatic Degassing During Eruptions

Gases released in phases 3 and 6 follow the pulses of deep magmatic gases (phases 2 and 5) and are closely associated with eruptive activity (Figure 2). These emissions are characterized by low CO_2/S_t, in the range of 1–2 on average (Figure 6), which is in agreement with regional trends in magmatic gas ratios [*Aiuppa et al.,* 2014; *Moussallam et al.,* 2014]. Comparison with degassing model outputs (Figure 6) indicates that these syneruptive CO_2-poor gases originate from magmatic degassing at far shallower conditions (150–75 MPa; 3–5 km) than during phases 2 and 5.

Importantly, the gases released during the first eruptive episode initiated by the 29 October 2014 eruption (phase 3) show a distinct gas composition in terms of H_2S/SO_2 from phase 6. The first eruptive episode shows average H_2S/SO_2 of 0.3, which is about an order of magnitude higher than the average H_2S/SO_2 measured after mid-March 2015 (phase 6). Following the modeling methods of *de Moor et al*. [2013b], we calculate that at expected magmatic conditions (QFM +1 to +3 and 900 to 1100°C) the magmatic H_2S/SO_2 ratio at outlet pressure should be in the range of 2×10^{-6} (high T and high fO_2) to 0.06 (low T and low fO_2). Thus, the first eruptive episode may have involved a minor hydrothermal component. Alternatively, gas released during the first eruptive episode may have been magmatic gas equilibrated at lower temperature than the magmatic gas released during the second eruptive episode. Assuming an fO_2 of QFM +1, the average H_2S/SO_2 of 0.3 measured during the first phase would indicate gas equilibration temperature of ~800°C, whereas the H_2S/SO_2 of $<$0.03 during the second period of eruptions implies gas equilibration temperatures of $>$950°C.

The gas emission rates from the two eruptive episodes were also very different. The phase 3 eruptions were preceded by a period of low gas flux, suggesting that degassing pathways were blocked. This concept is supported by field evidence, as the 29 October explosion erupted blocks of highly indurated hydrothermal breccia (Figure S3), which have not been observed in deposits from the latter eruptions. The matrix of these breccias consists of fine rock clasts with intense hydrothermal mineralization, which causes decreased permeability and self sealing that can inhibit the release of hydrothermal vapor and magmatic gas [e.g., *Christenson et al.,* 2010; *Sillitoe*, 2010]. These types of breccias are common in porphyry deposits, often form diatremes that cross-cut large volumes of intense hydrothermal alteration and mineralization and can transport hydrothermally altered clasts for $>$ 1 km vertically [*Sillitoe*, 2010]. The expulsion of the hydrothermal seal by the 29 October 2014 eruption was followed by the highest gas fluxes observed at Turrialba to date (Figure 2).

5.3.3. The Influence of the Hydrothermal System

The influence of the hydrothermal system is potentially manifested in a variety of ways: (1) modification of the composition of gases passing through the hydrothermal system after gas separation from magma, (2) scrubbing of reactive gases by interaction with meteoric/hydrothermal water, (3) addition of volatiles through boiling off of hydrothermal liquids and sublimation/combustion of hydrothermal minerals, and (4) changes to the permeability of the upper volcanic system.

The influence of the hydrothermal system at Turrialba is clearly demonstrated through the abundance of H_2S in the gas emissions during phases 1 and 4. The dominance of H_2S over SO_2 cannot be explained by magmatic degassing conditions at reasonable redox and temperature conditions for an arc-like magma [e.g., *de Moor et al.,* 2013b], and any H_2S/SO_2 ratio greater than 0.3 is considered hydrothermally influenced (Figure 3), pointing to reactions involving magmatic SO_2 and hydrothermal fluids.

One mechanism to produce H_2S is by disproportionation of SO_2 [e.g., *Kusakabe et al.,* 2000]:

$$4SO_{2(g)} + 4H_2O_{(l)} \rightarrow H_2S_{(g)} + 3H_2SO_{4(aq)} \quad (1)$$

This reaction is commonly called upon to explain scrubbing of SO_2 by hydrothermal systems, which would be expected to lower SO_2 flux, increase H_2S/SO_2, and also increase CO_2/S_t through bulk removal of S from the gas phase. At Turrialba, this reaction was probably significant during phase 1 passive degassing, where SO_2 fluxes were relatively low and H_2S/SO_2 and CO_2/S_t were slowly increasing. However, in general, the CO_2/S_t during hydrothermal phases 1 and 4 is only slightly higher than that of the shallow magmatic gases, suggesting that scrubbing by the hydrothermal system was not very efficient, most likely due to the strong gas flux and availability of relatively dry degassing pathways (i.e., 2010 and 2012 vents).

Alternatively, stored hydrothermal sulfur can be released during volcano reactivation, either as H_2S or SO_2 [*de Moor et al.,* 2005; *Giggenbach*, 1987; *Oppenheimer*, 1996]. Gases in moderate to high-temperature hydrothermal systems are usually saturated with respect to elemental sulfur [e.g., *Delmelle et al.,* 2000]:

$$SO_2 + 2H_2S \rightarrow 3S_0 + 2H_2O \quad (2)$$

Heating of the hydrothermal system and previously deposited native S drives this reaction to the left, resulting in 2 mol of H_2S and 1 mol of SO_2 for every 3 mol of elemental S consumed, with an expected H_2S/SO_2 ratio of 2 or similar to the maximum H_2S/SO_2 observed in the intense degassing period following phase 3 eruptions. Combustion of native S has also been directly observed in the field (burning native sulfur in the west crater), presenting evidence that a further hydrothermal contribution to the gas emissions is derived from

$$S_{0(s,l)} + O_{2(g,\,aq)} \rightarrow SO_{2(g)} \quad (3)$$

under shallow to surficial oxidizing conditions. In this case, oxygen can either be supplied from air or from air saturated meteoric water. Alternatively, under deeper reducing conditions a potential reaction would be

$$S_0 + H_2 \rightarrow H_2S \quad (4)$$

as H_2 is a significant component of hydrothermal and magmatic gases at Turrialba [*Vaselli et al.,* 2010].

Acidification of hydrothermal aquifers is yet another mechanism that could liberate stored volatiles. Hyperacid hydrothermal fluids (such as pH $<$ 1 volcanic lakes) can be almost transparent to volcanic gases [*Capaccioni et al.,* 2016; *de Moor et al.,* 2016; *Tamburello et al.,* 2015], whereas less extreme hydrothermal conditions significantly scrub acidic volcanic gases [e.g., *Symonds et al.,* 2001]. Thus, as a hydrothermal reservoir experiences more acidic magmatic gas input, it may release dissolved volatiles such as sulfur and chlorine.

Importantly, at Turrialba the total gas flux was highest during period 4, which was also a period of high H_2S/SO_2 values. The coincidence of very high gas flux and high H_2S/SO_2 probably reflects large-scale S expulsion from the hydrothermal system after shallow magma intrusion, degassing, and heat transfer during phase 3. Interestingly, the expulsion of the hydrothermal system is also accompanied by high CO_2 fluxes (Figure 2). The large CO_2 fluxes observed during phase 4 could thus partially represent remobilization of CO_2 stored chemically or physically in the hydrothermal system [*Chiodini et al.,* 2015; *Dawson et al.,* 2016].

Volatiles can be trapped in volcanic edifices chemically in hydrothermal fluids (dissolved S or C species) or as hydrothermal minerals (e.g., native sulfur, sulfides, sulfates, and carbonates). Additionally, gases can be

Table 2. Sulfur Budget and Magma Volume Calculations for Turrialba, Calculated Based on Flux Monitoring Data Since 2008

SO_2 Emitted (t)	H_2S Emitted[a] (t)	Total S Emitted (t)	Melt S Content (wt %)	Mass Melt Degassed (kg)	Magma Volume (km^3)
2.04×10^6	6.12×10^5	1.60×10^6	0.2	7.99×10^{11}	0.296

[a]The average H_2S/SO_2 ratio of 0.6 from Multi-GAS data (Figure 2) is assumed in order to estimate total H_2S emissions.

physically trapped below low permeability hydrothermal seals [e.g., *Christenson et al.,* 2010]. Blocked conduits can lead to pressurization below hydrothermal seals and explosive eruption. Phase 2 demonstrates low gas fluxes suggesting sealing of the shallow conduits prior to the 29 October eruption (Figure S3), providing a reasonable explanation for the explosivity of that blast. After this eruption and intense volcano tectonic seismicity and fracturing, the permeability of the volcanic edifice increased significantly, allowing the expulsion of hydrothermally stored volatiles during phase 4. A second deep magmatic pulse was superimposed on this ongoing process during phase 5, and hydrothermal volatiles were still involved in the first eruptions of phase 6. These eruptions were most likely associated with the rise of a magma pulse into the shallow plumbing system and opening of new conduits that allowed high-temperature magmatic gas ($H_2S/SO_2 << 0.3$) to reach the surface without hydrothermal interaction.

6. Evolution of the Eruptive Activity and Implications

Since the first ash eruption at Turrialba in 2010, the key questions have been whether a new magma body is rising to the surface, whether and how a magmatic eruption will occur and for how long the eruptive activity will continue. By summing averaged daily gas flux measurements, we estimate that Turrialba has released ~2.04 Mt (megatons) of SO_2 through persistent degassing since 2008, which suggests emplacement of new magmatic intrusions of ~0.3 km^3 in total (Table 2). A negligible volume of this magma has been erupted, as the new ashes are still dominated by altered material, and the ash volumes erupted are too small to accurately constrain in a meaningful sense. In comparison, *Reagan et al.* [2006] estimated an eruptive volume of <0.03 km^3 for the 1864–1866 eruption products.

In conjunction with continuous inflation since 2010 and increasing component of fresh-looking magmatic clasts, voluminous degassing strongly suggests intrusion of new magma. However, the amount of gas emitted per se gives no indication of the timing of gas separation from the magma, and as such (without strong independent evidence such as inflation) there remains the possibility that gas has been accumulated in the crust over tens to thousands of years during slow magma crystallization [*Christopher et al.,* 2015]. Indeed, our data do suggest that large volumes of volatiles were stored in the hydrothermal system and released in phase 4 following the 29 October 2014 eruption. Degassed melt inclusions with more evolved compositions than matrix glass further point to the possibility that old, previously degassed (but still mobile) magma is involved (either passively or actively) in eruptions at Turrialba, perhaps suggesting that some of the emitted gas could also be remnant from previous intrusions (pre-1866). Instability in a system of accumulated magmatic gas beneath a well-sealed hydrothermal system could conceivably cause small phreatic eruptions that do not lead to large and explosive magmatic eruption. However, gas compositional changes consistent with repetitive magma decompression events provides strong support for a model involving magma batches rising from the deep to shallow crust (Figure 7). Our data do suggest that a significant (but unquantifiable) portion of the total emitted sulfur is remobilized from the hydrothermal system, which could potentially store volatiles for considerable periods of time between eruptive episodes. Therefore, the estimation of new intruded magma volume based on sulfur emissions should be considered a maximum, as a proportion of the emitted sulfur may not be directly degassed by the rising magma bodies but rather be stored hydrothermal sulfur remobilized during reactivation of the volcano.

Monitoring of multiple gas components allows us to see through the hydrothermal overprint in the gas signatures and recognize two cycles of magmatic degassing (phases 1–3 and phases 4–6), progressing from deep magmatic CO_2-rich gas to shallow magmatic SO_2-rich gas, which is accompanied by eruptive activity. High-frequency monitoring of volcanic gas compositions allowed by technological advances in the last decade is repeatedly showing the value of these measurements in forecasting and understanding volcanic eruptions [*Aiuppa et al.,* 2007; *Burton et al.,* 2007; *de Moor et al.,* 2016; *Oppenheimer et al.,* 2011]. Modeling of the

compositional trends strongly suggests decompression degassing of pulses of magma arriving from deep to shallow crustal levels. The variations are not consistent with a single volatile source of old stored magmatic gas, as logically this would be expected to be compositionally homogenous without major variations related to pressure dependent gas solubility in melt.

Ash deposits erupted over the measurement period are all dominated by hydrothermally altered material; however, there has been discussion on whether there is juvenile material present in the ash or not since the first eruption in Turrialba in 2010 [*Reagan et al.,* 2011], a discussion which entered the public forum (http://www.ticotimes.net/2015/03/13/costa-ricas-turrialba-volcano-appears-to-erupt-lava; http://www.ticotimes.net/2015/04/11/possible-lava-rocks-indicate-turrialba-volcano-may-have-entered-more-dangerous-phase) and has even reached high levels of Costa Rican government. The composition of the fresh glassy component in these complex ash samples is similar to that of magmatic clasts derived from the 1864–1866 eruption (Figures 4 and 5) leaving us with the seemingly irreconcilable conundrum (at least geochemically speaking) of whether this material represents erosion of old magmatic (or phreatomagmatic) deposits or newly quenched magma reaching the surface.

Our high-frequency gas composition data, the first reported for vent-opening eruptions, demonstrate that the transition from phreatic to phreatomagmatic activity can be monitored using in situ multi-GAS, providing a reliable, near real time, and safe indication of the transition from hydrothermally influenced to magmatically dominated eruptive conditions. The gas compositions as measured by multi-GAS demonstrate a first-order change from hydrothermal (presence of H_2S) to magmatic (H_2S/SO_2 close to zero) over the period of unrest. The unambiguous change in gas chemistry combined with deformation monitoring convincingly argue for rising magma that has established open vents to the surface. Using the abrupt change in H_2S/SO_2, we propose that the transition from "phreatic" to "phreatomagmatic" dominated conditions occurred between 17 and 20 March. Based on the combined gas and deformation data (Figure S2), it seems likely that the fresh clasts in the recent ashes do, in fact, represent new magma arriving at the surface.

The general similarity in the progression of the activity and the observation that the composition of the fresh component in the ash is similar to that of the 1864–1866 eruption suggests that it is reasonable to use the previous eruption as a model for preparation plans for the current crisis. If so, the current eruptions are probably reflecting a similar transition from phreatic to phreatomagmatic as that recorded in geological record. If the progression of eruptive activity continues in a similar fashion to the 1864–1866 eruption [*González et al.,* 2015], continued eruptive activity would be expected in the future, perhaps terminating with magmatic eruptions producing material similar in composition to the 1864–1866 eruption (this work). The volume of gas released from Turrialba suggests the intrusion of a volume (0.3 km^3) of the same order of magnitude to that driving the1864–1866 eruption ($<$0.03 km^3 erupted), because arc magmas typically release about an order of magnitude more gas than can be supplied by the amount of erupted magma [e.g., *Wallace and Edmonds*, 2011]. However, we cannot exclude the possibility that the magma body stalls and fails to erupt [*Moran et al.,* 2011] or that a more silicic and voluminous eruption (such as the 2000 ka subplinian eruption) [*Reagan et al.,* 2006] takes place. Furthermore, a significant portion of the sulfur emitted from Turrialba from 2008 to present could have been remobilized from an extensive hydrothermal system, as is exemplified by high SO_2 flux and H_2S/SO_2 during phase 4 degassing (Figure 2).

Recent studies have also shown that large reservoirs of carbon can be stored in and released from hydrothermal systems [*Chiodini et al.,* 2015; *Dawson et al.,* 2016]. During the period of study (June 2014 to April 2015) we estimate that a total of ~0.86 Mt of CO_2 has been released from Turrialba based on daily calculated CO_2 fluxes. Of this total, ~0.52 Mt of CO_2 was released during phase 4 degassing, which followed breaking of the hydrothermal seal by the 29 October eruption, and is associated with hydrothermal values of H_2S/SO_2. Thus, a significant proportion of volcanic CO_2 may be accumulated beneath hydrothermally sealed carapaces and released after relatively small vent-opening eruptions at volcanoes with extensive and long-lived hydrothermal systems.

7. Conclusion

Turrialba Volcano continues to represent a significant and growing threat to the society and economy of Costa Rica. Here we show that periods of activity are due to the arrival of distinct magma batches from the deep crust to a shallow crustal magma reservoir. CO_2-rich gas pulses derived from deep degassing occur

before eruptive episodes, and ash emissions are accompanied by shallow magmatic degassing. The hydrothermal system has continued to play a significant role in voluminous volcanic degassing at Turrialba over a more than a decade of unrest.

The transition from phreatic to phreatomagmatic eruptive behavior is a fundamental change in any evolving volcanic crisis. The reactivation of Turrialba has been an extraordinarily slow progression, allowing detailed study of the evolution toward magmatic conditions at a volcano with an extensive hydrothermal system. Phreatomagmatic eruptions tend be more violent and prolonged, and emit fine ash that can travel long distances [*Morrissey et al.,* 2000; *Nakada et al.,* 1995]. Here we have shown that volcanic gas monitoring can be used to identify this transition, which is quicker, safer, and less ambiguous than ash component analyses. Specifically, high-frequency monitoring of H_2S/SO_2 is a valuable parameter for assessing the relative contributions of hydrothermal and magmatic sources during eruptive crises. Variations in these contributions can be large and occur rapidly. At Turrialba, the transition from hydrothermal to purely magmatic degassing took place between 17 and 20 March, which coincided with numerous disruptions to air traffic at San José International Airport (12, 21, and 23 March and 4 and 18 May). If phreatomagmatic eruptions continue at Turrialba, the tourism-based economy of Costa Rica will suffer. Numerous examples from the past decade show that high-frequency monitoring of volcanic gases is consistently revealing important new insights into eruptive behavior with clear implications for volcanic hazard assessment.

Acknowledgments

Taryn Lopez and Dmitri Rouwet are thanked for thoughtful reviews of this article. Christoph Kern and VDAP are thanked for support with DOAS instrumentation. OVSCORI personnel are thanked for field and logistical support. Viorel Atudorei and Zach Sharp are thanked for use of the stable isotope lab at UNM and analytical guidance. Martyn Keizer is thanked for setting up an online tool for the public to report ash emissions. J.M.d.M. thanks Tobias Fischer for many years of mentorship and introducing him to Turrialba Volcano in 2009. We wish to thank Kaj Hoernle, Paul van den Bogaard, Seth Sadofsky, and Carlos Ramírez for providing the tephra sample from the 1865 eruption, obtained during a field campaign of Sonderforschungsbereich 574, funded by the German Research Foundation (DFG). This research was funded by the Costa Rican Comision Nacional de Emergencias, the Deep Carbon Observatory, and the European Research Council (FP7/ERC grant agreement 305377). All data are available in the supporting information.

References

Aiuppa, A., R. Moretti, C. Federico, G. Giudice, S. Gurrieri, M. Liuzzo, P. Papale, H. Shinohara, and M. Valenza (2007), Forecasting Etna eruptions by real-time observation of volcanic gas composition, *Geology*, *35*, 1115–1118.

Aiuppa, A., C. Federico, G. Giudice, G. Giuffrida, R. Guida, S. Gurrieri, M. Liuzzo, R. Moretti, and P. Papale (2009), The 2007 eruption of Stromboli Volcano: Insights from the real-time measurement of the volcanic gas plume CO_2/SO_2 ratio, *J. Volcanol. Geotherm. Res.*, *182*, 221–230.

Aiuppa, A., P. Robidoux, G. Tamburello, V. Conde, B. Galle, G. Avard, E. Bagnato, J. M. De Moor, M. Martinez, and A. Muñóz (2014), Gas measurements from the Costa Rica-Nicaragua volcanic segment suggest possible along-arc variations in volcanic gas chemistry, *Earth Planet. Sci. Lett.*, *407*, 134–147.

Alvarado, G. E. (1993), Volcanology and Petrology of Irazu Volcano, Costa Rica, PhD thesis, 289 pp., University of Kiel, Kiel.

Alvarado, G. E. (2009), *Los Volcanes de Costa Rica: Geología, Historia, Riqueza Natural y du Gente*, 3rd ed., Editorial Universidad Estatal a Distancia, San José, Costa Rica.

Baker, D. R., and R. Moretti (2011), Modeling the solubility of sulfur in magmas: A 50-year old geochemical challenge, in *Sulfur in Magmas and Melts: Its Importance for Natural and Technical Processes*, *Geochem. Soc., Rev. Mineral. Geochem.*, vol. 73, edited by H. Behrens and J. D. Webster, pp. 167–213, Mineralogical Society of America, Washington.

Barberi, F., A. Bertagnini, P. Landi, and C. Principe (1992), A review on phreatic eruptions and their precursors, *J. Volcanol. Geotherm. Res.*, *52*, 231–246.

Benjamin, E. R., T. Plank, J. A. Wade, K. A. Kelley, E. H. Hauri, and G. E. Alvarado (2007), High water contents in basaltic magmas from Irazú Volcano, Costa Rica, *J. Volcanol. Geotherm. Res.*, *168*, 68–92.

Burton, M., P. Allard, F. Murè, and A. La Spina (2007), Depth of slug-driven strombolian explosive activity, *Science*, *317*, 227–230.

Campion, R., M. Martinez-Cruz, T. Lecocq, C. Caudron, J. Pacheco, G. Pinardi, C. Hermans, S. Carn, and A. Bernard (2012), Space- and ground-based measurements of sulphur dioxide emissions from Turrialba Volcano (Costa Rica), *Bull. Volcanol.*, *74*, 1757–1770.

Capaccioni, B., D. Rouwet, and F. Tassi (2016), HCl degassing from extremely acidic crater lakes: Preliminary results from experimental determinations and implications for geochemical monitoring, *Geol. Soc. Lond. Spec. Publ.*, *437*, doi:10.1144/SP437.12.

Carr, M. J., and R. E. Stoiber (1990), Volcanism, in *The Caribbean Region. The Geology of North America*, edited by G. Dengo and J. E. Case, pp. 375–391, Geol. Soc. Am., Boulder, Colo.

Cashman, K. V., and R. P. Hoblitt (2004), Magmatic precursors to the 18 May 1980 eruption of Mount St. Helens, USA, *Geology*, *32*, 141–144.

Chiodini, G., L. Pappalardo, A. Aiuppa, and S. Caliro (2015), The geological CO_2 degassing history of a long-lived caldera, *Geology*, *43*, 767–770, doi:10.1130/G36905.36901.

Christenson, B. W., A. G. Reyes, R. Young, A. Moebis, S. Sherburn, J. Cole-Baker, and K. Britten (2010), Cyclic processes and factors leading to phreatic eruption events: Insights from the 25 September 2007 eruption through Ruapehu Crater Lake, New Zealand, *J. Volcanol. Geotherm. Res.*, *191*, 15–32.

Christopher, T. E., J. Blundy, K. Cashman, P. Cole, M. Edmonds, P. J. Smith, R. S. J. Sparks, and A. Stinton (2015), Crustal-scale degassing due to magma system destabilization and decoupling at Soufrière Hills Volcano, Monteserrat, *Geochem. Geophys. Geosyst.*, *16*, 2797–2811, doi:10.1002/2015GC005791.

Claiborne, L. L., C. F. Miller, D. M. Flanagan, M. A. Clynne, and J. L. Wooden (2010), Zircon reveals protracted magma storage and recycling beneath Mount St. Helens, *Geology*, *38*, 1011–1014.

Conde, V., S. Bredemeyer, E. Duarte, J. Pacheco, S. Miranda, B. Galle, and T. H. Hansteen (2013), SO_2 degassing from Turrialba Volcano linked to seismic signatures during the period 2008–2012, *Int. J. Earth Sci.*, doi:10.1007/s00531-00013-00958-00535.

Dawson, P., B. Chouet, and A. C. J. B. Pitt (2016), Tomographic image of a seismically active volcano: Mammoth Mountain, California, *J. Geophys. Res. Solid Earth*, *121*, 114–133, doi:10.1002/2015JB012537.

de Moor, J. M., T. P. Fischer, D. R. Hilton, E. Hauri, L. A. Jaffe, and J. T. Camacho (2005), Degassing at Anatahan Volcano during the May 2003 eruption: Implications from petrology, ash leachates, and SO_2 emissions, *J. Volcanol. Geotherm. Res.*, *146*, 117–138.

de Moor, J. M., T. P. Fischer, P. L. King, and Z. D. Sharp (2013a), The sulfur cycle at subduction zones, Abstract V41E-07 presented at 2013 Fall Meeting, AGU, San Francisco, Calif., 9–13 Dec.

de Moor, J. M., et al. (2013b), Sulfur degassing at Erta Ale (Ethiopia) and Masaya (Nicaragua): Implications for degassing processes and oxygen fugacities of basaltic systems, *Geochem. Geophys. Geosyst.*, *14*, 4076–4108, doi:10.1002/ggge.20255.

de Moor, J. M., A. Aiuppa, J. Pacheco, G. Avard, C. Kern, M. Liuzzo, M. Martinez, G. Giudice, and T. P. Fischer (2016), Short-period volcanic gas precursors to phreatic eruptions: Insights from Poás Volcano, Costa Rica, *Earth Planet. Sci. Lett.*, *442*, 218–227, doi:10.1016/j.epsl.2016.1002.1056.

Delmelle, P., A. Bernard, M. Kusakabe, T. P. Fischer, and B. Takano (2000), Geochemistry of the magmatic-hydrothermal system of Kawah Ijen Volcano, East Java, Indonesia, *J. Volcanol. Geotherm. Res.*, *97*, 31–53.

Di Piazza, A., A. L. Rizzo, F. Barberi, M. L. Carapezza, G. D. Astis, and C. Romano (2015), Geochemistry of the mantle source and magma feeding system beneath Turrialba Volcano, Costa Rica, *Lithos*, *232*, 319–335.

Galle, B., M. Johansson, C. Rivera, Y. Zhang, M. Kihlman, C. Kern, T. Lehmann, U. Platt, S. Arellano, and S. Hidalgo (2010), Network for Observation of Volcanic and Atmospheric Change (NOVAC)—A global network for volcanic gas monitoring: Network layout and instrument description, *J. Geophys. Res.*, *115*, D05304, doi:10.1029/2009JD011823.

Gazel, E., M. J. Carr, K. Hoernle, M. D. Feigenson, D. Szymanski, F. Hauff, and P. C. Q. S. van den Bogaard (2009), Galapagos-OIB signature in southern Central America: Mantle refertilization by arc–hot spot interaction, *Geochem. Geophys. Geosyst.*, *10*, Q02S11, doi:10.1029/2008GC002246.

Giggenbach, W. F. (1987), Redox processes governing the chemistry of fumarolic gas discharges from White Island, New Zealand, *Appl. Geochem.*, *2*, 143–161.

Giggenbach, W. F. (1996), Chemical composition of volcanic gas, in *IAVCEI-UNESCO: Monitoring and Mitigation of Volcanic Hazards*, edited by R. Tilling, pp. 221–256, Springer, Berlin.

Giggenbach, W. F., N. Garcia, A. Londoño, L. Rodriguez, N. Rojas, and M. L. Calvache (1990), The chemistry of fumarolic vapor and thermal-spring discharges from the Nevado del Ruiz volcanic-magmatic-hydrothermal system, Colombia, *J. Volcanol. Geotherm. Res.*, *42*, 13–39.

González, G., R. Mora-Amador, C. Ramírez, D. Rouwet, A. Yemerith, C. Picado, and R. Mora (2015), Actividad historica y analisis de la amenaza del volcan Turrialba, Costa Rica, *Rev. Geol. Am. Central*, *52*, 129–149.

Holloway, J. R., and J. G. Blank (1994), Application of experimental results to C-O-H species in natural melts, in *Volatiles in Magmas*, edited by M. R. Carroll and J. R. Holloway, pp. 187–230, Mineralogical Society of America, Fredericksburg.

Kusakabe, M., Y. Komoda, B. Takano, and T. Abiko (2000), Sulfur isotopic effects in the disproportionation reaction of sulfur dioxide in hydrothermal fluids: Implications for the delta S-34 variations of dissolved bisulfate and elemental sulfur from active crater lakes, *J. Volcanol. Geotherm. Res.*, *97*, 287–307.

Larsen, J. F., C. J. Nye, M. L. Coombs, M. Tilman, P. Izbekov, and C. Cameron (2010), Petrology and geochemistry of the 2006 eruption of Augustine Volcano, in *The 2006 Eruption of Augustine Volcano*, *U.S. Geol. Surv. Prof. Pap.*, edited by J. A. Power et al., pp. 335–382.

Lesne, P., S. C. Kohn, J. Blundy, F. Witham, R. E. Botcharnikov, and H. Behrens (2011), Experimental simulation of closed-system degassing in the system basalt-H_2O-CO_2-S-Cl, *J. Petrol.*, *52*, 1737–1762.

Martini, F., F. Tassi, O. Vaselli, R. Del Potro, M. Martinez, R. Van del Laat, and E. Fernandez (2010), Geophysical, geochemical and geodetical signals of reawakening at Turrialba Volcano (Costa Rica) after almost 150 years of quiescence, *J. Volcanol. Geotherm. Res.*, *198*, 416–432.

Moran, S. C., C. Newhall, and D. C. Roman (2011), Failed magmatic eruptions: Late-stage cessation of magma ascent, *Bull. Volcanol.*, *73*, 115–122.

Moretti, R., P. Papale, and G. Ottonello (2003), A model for the saturation of C-H-O-S fluids in silicate melts, in *Volcanic Degassing*, edited by C. Oppenheimer et al., pp. 81–101, Geol. Soc. Lond. Spec. Publ, London.

Morrissey, M., B. Zimanowski, K. Wohletz, and R. Buettner (2000), Phreatomagmatic fragmentation, in *Encyclopedia of Volcanoes*, edited by H. Sigurdsson, pp. 431–445, Academic Press, New York.

Moussallam, Y., N. Peters, C. Ramirez, C. Oppenheimer, A. Aiuppa, and G. Giudice (2014), Characterisation of the magmatic signature in gas emissions from Turrialba Volcano, Costa Rica, *Solid Earth*, *6*, 2293–2320.

Nakada, S., Y. Motomura, and H. Shimizu (1995), Manner of magma ascent at Unzen Volcano (Japan), *Geophys. Res. Lett.*, *22*, 567–570, doi:10.1029/95GL00002.

Oppenheimer, C. (1996), On the role of hydrothermal systems in the transfer of volcanic sulfur to the atmosphere, *Geophys. Res. Lett.*, *23*, 2057–2060, doi:10.1029/96GL02061.

Oppenheimer, C., R. Moretti, P. R. Kyle, A. Eschenbacher, J. B. Lowenstern, R. L. Hervig, and N. W. Dunbar (2011), Mantle to surface degassing of alkalic magmas at Erebus Volcano, Antarctica, *Earth Planet. Sci. Lett.*, *306*, 261–271.

Oppenheimer, C., T. P. Fischer, and B. Scaillet (2012), Volcanic degassing: Process and impact, in *The Crust, Treatise on Geochemistry*, edited by H. D. Holland et al., pp. 111–179, Elsevier-Pergamon, Oxford.

Pardo, N., et al. (2014), Perils in distinguishing phreatic from phreatomagmatic ash; insights into the eruption mechanisms of the 6 August 2012 Mt. Tongariro eruption, New Zealand, *J. Volcanol. Geotherm. Res.*, *286*, 397–414.

Peacock, S. M., P. E. van Keken, S. D. Holloway, B. R. Hacker, G. A. Abers, and R. L. Fergason (2005), Thermal structure of the Costa Rica-Nicaragua subduction zone, *Phys. Earth Planet. Int.*, *149*, 187–200.

Reagan, M., E. Duarte, G. J. Soto, and E. Fernandez (2006), The eruptive history of Turrialba Volcano, Costa Rica, and potential hazards from future eruptions, in *Volcanic hazards in Central America*, edited by W. I. Rose et al., *Geol. Soc. Am. Spec. Pap.*, pp. 235–257.

Reagan, M., M. Rowe, E. Duarte, and E. Fernández (2011), Juvenile glass fragments in phreatic explosion debris from Turrialba Volcano, Costa Rica, paper presented at Goldschmidt Conf. Abstracts, Mineral Magazine, Prague.

Ruprecht, P., and T. Plank (2013), Feeding andesitic eruptions with a high-speed connection from the mantle, *Nature*, *500*, 68–72.

Shaw, A. M., D. R. Hilton, T. P. Fischer, J. A. Walker, and G. E. Alvarado (2003), Contrasting He-C relationships in Nicaragua and Costa Rica: Insights into C cycling through subduction zones, *Earth Planet. Sci. Lett.*, *214*, 499–513.

Sillitoe, R. H. (2010), Porphyry Copper Systems, *Econ. Geol.*, *105*, 3–41.

Spadaro, F., R. Lefèvre, and P. Ausset (2002), Experimental rapid alteration of basaltic glass: Implications for the origins of atmospheric particulates, *Geology*, *30*, 671–674.

Suzuki, Y., M. Nagai, F. Maeno, A. Yasuda, N. Hokanishi, T. Shimano, M. Ichihara, T. Kaneko, and S. Nakada (2013), Precursory activity and evolution of the 2011 eruption of Shinmoe-dake in Kirishima Volcano—Insights from ash samples, *Earth Planets Space*, *65*, 591–607.

Symonds, R. B., T. M. Gerlach, and M. H. Reed (2001), Magmatic gas scrubbing: Implications for volcano monitoring, *J. Volcanol. Geotherm. Res.*, *108*, 303–341.

Tamburello, G., et al. (2015), Intense magmatic degassing through the lake of Copahue Volcano, 2013–2014, *J. Geophys. Res. Solid Earth*, *120*, 6071–6084, doi:10.1002/2015JB012160.

Vaselli, O., F. Tassi, E. Duarte, E. Fernandez, R. J. Poreda, and A. Huertas (2010), Evolution of fluid geochemistry at the Turrialba Volcano (Costa Rica) from 1998 to 2008, *Bull. Volcanol.*, *72*, 397–410.

Wallace, P. J., and M. Edmonds (2011), The sulfur budget in magmas: Evidence from melt inclusions, submarine glasses, and volcanic gas emissions, in *Sulfur in Magmas and Melts: Its Importance for Natural and Technical Processes*, edited by H. Behrens and J. D. Webster, pp. 215–246, The Mineralogical Society of America, Chantilly, Va.

Wehrmann, H., K. Hoernle, M. Portnyagin, M. Wiedenbeck, and K. Heydolph (2011), Volcanic CO_2 output at the Central American subduction zone inferred from melt inclusions in olivine crystals from mafic tephras, *Geochem. Geophys. Geosyst.*, *12*, Q06003, doi:10.1029/2010GC003412.

Williams, S. N., R. E. Stoiber, N. P. Garcia, A. C. Londoño, B. Gemmell, D. R. Lowe, and C. B. Connor (1986), Eruption of the Nevado del Ruiz Volcano, Colombia, on 13 November 1985: Gas flux and fluid Geochemistry, *Science*, *233*, 964–967.